

Sensitivity of the tropical Pacific Ocean simulation to the temporal and spatial resolution of wind forcing

Dake Chen

Lamont-Doherty Earth Observatory, Columbia University, Palisades, New York

W. Timothy Liu

Jet Propulsion Laboratory, Pasadena, California

Stephen E. Zebiak, Mark A. Cane, Yochanan Kushnir, and Donna Witter

Lamont-Doherty Earth Observatory, Columbia University, Palisades, New York

Abstract. The effects of temporal and spatial smoothing of wind forcing were evaluated in a model simulation of the tropical Pacific Ocean variability during the onset phase of the 1997/1998 El Niño. A total of 16 experiments were performed using the NASA scatterometer wind data smoothed at time intervals from 1 to 30 days and on spatial scales from 1° to 10°. A major effect of the temporal smoothing of winds is to warm sea surface temperature (SST) by reducing the energy input for vertical turbulent mixing. When the daily wind forcing was replaced by the monthly average, the mean SST increased by 0.5° to 1° over most of the tropical Pacific. The spatial smoothing of winds is not as effective as the temporal smoothing in causing SST warming, but it has a more severe influence on dynamical ocean response for smoothing scales above 5°. The onset of the 1997/1998 El Niño can be successfully simulated using the wind forcing averaged to monthly intervals and 2° squares. For climate models the spatial smoothing of wind forcing on scales larger than the width of the equatorial waveguide is a more serious limitation than the temporal smoothing on scales up to 1 month.

1. Introduction

The upper ocean dynamical and thermal structures are largely determined by the wind forcing at the ocean surface. Thus the numerical ocean models that attempt to simulate these structures have to include a good representation of wind stress as a surface boundary condition. However, because of the general lack of wind observations over the ocean, modelers usually have no choice but to resort to the wind products with relatively coarse spatial and temporal resolution. For example, the commonly used Florida State University (FSU) wind analysis [Goldenberg and O'Brien, 1981] is monthly in time and virtually 2° latitude by 10° longitude in space, which is typical for wind analyses based mainly on shipboard observations. Although some high-resolution wind data from buoys have occasionally been used to drive small-scale ocean models for a limited period of time [e.g., Chen and Wang, 1990], large-scale climate models are invariably forced with low-resolution wind products such as the FSU analysis.

The underlying assumption of our common practice with low-resolution wind data is that high-frequency, small-scale winds have insignificant influence on the low-frequency, large-scale ocean variabilities. This might be true to some extent but is not likely to be generally applicable. For instance, using a quasi-geostrophic (QG) model of the North Pacific Ocean, Large *et al.* [1991] showed that high-frequency wind forcing accounts for a large portion of the barotropic ocean response

Copyright 1999 by the American Geophysical Union.

Paper number 1998JC900031.
0148-0227/99/1998JC900031\$09.00

and deep kinetic energy, although its effects on the baroclinic fields are quite small. Also in the context of a midlatitude QG model, Milliff *et al.* [1996] investigated the role of high-wavenumber wind forcing. They found that the mean and eddy kinetic energies could be enhanced by up to an order of magnitude in the eastern basin of the North Atlantic when the high-wavenumber forcing was applied. The sensitivity of ocean simulations to wind resolution has also been studied by investigators who were concerned with the impact of satellite scatterometer winds [Barnier *et al.*, 1991, 1994].

A potentially important aspect of the high-frequency, small-scale wind forcing that has not been addressed previously is its effects on the upper ocean thermal structure, especially sea surface temperature (SST), a vital parameter in ocean-atmosphere interaction. There are reasons to believe that these effects are far from negligible. First of all, winds can force turbulent mixing in the ocean surface layer. Because this diffusive process is irreversible, effects of high-frequency winds do not average out. The reason is that the energy for turbulence production depends on the magnitude, but not the direction, of winds. It has been demonstrated that a zero-mean, sinusoidal, high-frequency wind signal can significantly cool SST through vertical mixing, especially when mean winds are weak and the surface mixed layer is shallow [Chen *et al.*, 1994a]. In a model driven by annual or monthly mean winds, it is often necessary to set an artificial lower limit on wind magnitude to prevent the model from becoming too warm [e.g., Gent, 1991].

In addition to its local effects, high-frequency wind forcing can also remotely alter oceanic conditions by generating non-dispersive long waves, which is particularly true in the equato-

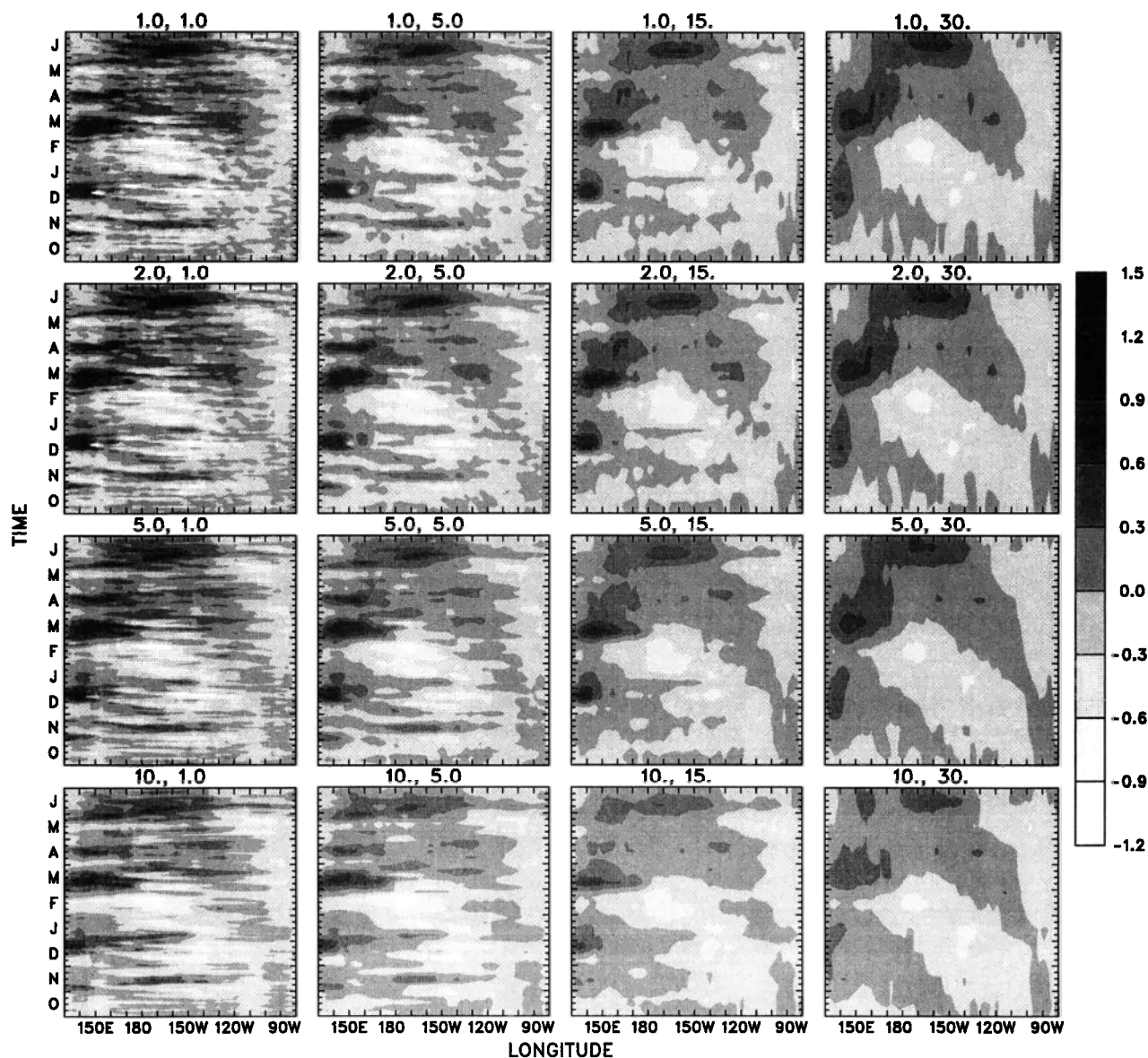


Figure 1. Longitude-time plots of the NASA scatterometer (NSCAT) zonal wind stress along the equator for 16 different resolutions, October 1996 to June 1997. The two numbers at top of each plot denote the grid size in degrees and the time period in days over which the wind data are averaged.

rial and coastal waveguides. Of special interest here are the energetic Kelvin waves generated by the westerly wind bursts in the western equatorial Pacific. These waves have a strong downstream influence on the central and eastern part of the ocean and arguably may play an important role in the onset of El Niño [Webster and Lukas, 1992; Kessler et al., 1995]. Since the westerly wind bursts have a duration of approximately 10 days, they could be smeared in monthly mean wind products, and the resulting Kelvin waves could be severely modified. It is not yet clear whether using monthly winds is sufficient for the climate models that aim at interannual or longer timescales. Intuitively, one might think that the predictive skill of El Niño models could be degraded by having only low-resolution winds for initialization, but this seems at odds with the general success of such models.

Therefore it is necessary to quantify the sensitivity of ocean response, in terms of both dynamical and thermal fields, to the wind forcing with different temporal and spatial resolutions. The forcing sets can be either synthesized from the weather

center analyses as in the studies mentioned above or, more realistically, constructed from real wind observations. The latter approach was not possible until recently, when satellite-derived high-resolution winds became available. In this study we chose to employ the NASA scatterometer (NSCAT) wind data, binned into different spatial grids and time intervals for the 9-month period from October 1996 to June 1997, to drive a primitive equation model of the tropical Pacific Ocean. Because the study period covers the onset phase of the 1997/1998 El Niño, during which the activities in the tropical Pacific were particularly rich, we were able to examine the impact of the wind-forcing resolution on various ocean variabilities, ranging from intraseasonal to interannual timescales.

2. Data and Model

The gridded wind fields used in this study are objectively interpolated from the NSCAT wind observations, with a tem-

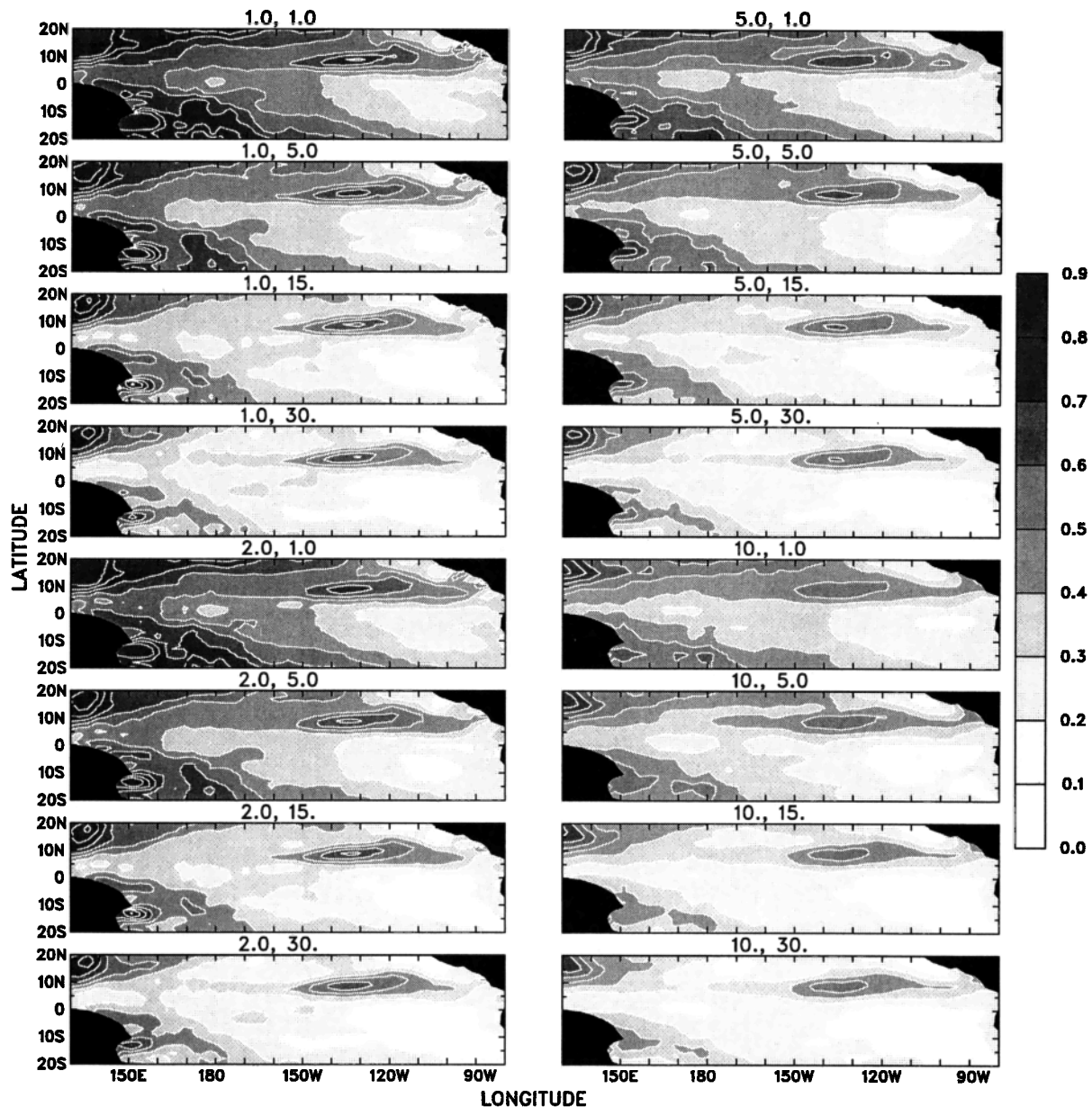


Figure 2. Standard deviation of the NSCAT wind stress magnitude from the climatological mean for 16 different resolutions. The numbers at top have the same meaning as in Figure 1.

poral resolution of 12 hours and a spatial resolution of 0.5° latitude by 0.5° longitude. The methodology of data processing is given by Liu *et al.* [1998]. Here we are not concerned with the accuracy of the NSCAT data and the impact of sampling strategy, which have been the focus of many other studies [e.g., Barnier *et al.*, 1991, 1994; Bourassa *et al.*, 1997]. Suffice it to say that the NSCAT wind product is probably the best resolved wind data set available and its quality is sufficient for the purpose of this study. Since our interest is to compare model experiments forced by differently smoothed versions of the same wind product, the errors in the original wind product should have little influence on our results reported here.

In order to construct a set of wind forcing with various temporal and spatial resolutions, we first averaged the data spatially into 1° , 2° , 5° , and 10° squares and then averaged them in time at intervals of 1, 5, 15, and 30 days, resulting in a total

of 16 different time series of wind stress fields. This simple approach is different from that of Large *et al.* [1991] and Milliff *et al.* [1996], who identified the forcing at different frequency and wavenumber bands by carefully filtering the data in the frequency and wavenumber domains. We are more interested in the effects of simple temporal and spatial smoothing rather than the ocean response to the wind forcing of specific frequencies and wavenumbers. Therefore aliasing is not a problem with which we need to be concerned. Our approach is useful since most low-resolution wind products available were obtained by simple temporal and spatial averaging.

The model used here is a version of the σ coordinate, primitive equation, reduced-gravity model developed by Gent and Cane [1989], within which the hybrid mixed layer model of Chen *et al.* [1994a] is embedded. The model was originally designed to support simulation and process studies of the trop-

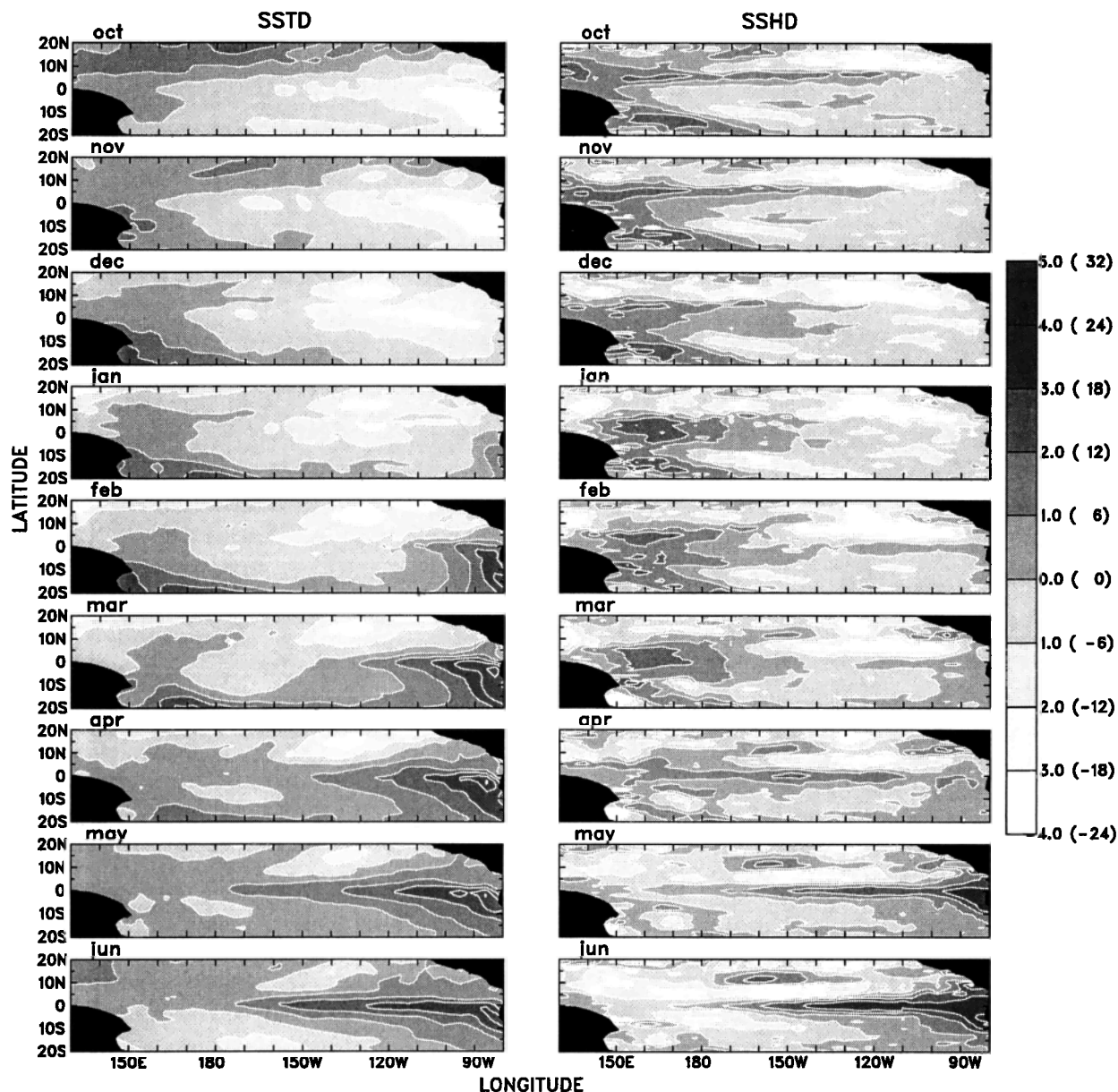


Figure 3. Monthly averaged observations of the sea surface temperature (SST) and sea level deviations from the 1993–1995 three-year mean, for the 9 months from October 1996 to June 1997.

ical oceans. It has been applied previously to simulating the mean circulation and the SST seasonal cycle in the tropical Pacific Ocean [Gent, 1991; Chen *et al.*, 1994a, b]. The model has seven layers in the vertical with higher resolution right below the mixed layer and a stretched grid in the horizontal with an average grid spacing of 1° . The meridional resolution is higher than 0.5° in the equatorial waveguide. The model domain extends from 120°E to 70°W and 30°S to 30°N . Within 10° of the southern and northern boundaries, temperature and salinity are gradually relaxed back to the Levitus [1982] climatology. The surface heat and freshwater fluxes are specified using climatological data as described by Chen *et al.* [1994b]. The model experiments discussed in section 3 differ from one another only in wind forcing.

3. Results

3.1. Wind Forcing

The model was spun up with the monthly FSU winds from January 1961 to September 1996, and then the FSU winds were gradually switched to the NSCAT winds over a period of 1 month. From October 1996 to June 1997 the model was run with the NSCAT winds of 16 different resolutions. Before we compare the results from these experiments, let us first take a look at the differences in the wind-forcing fields. For clarity we only examine the deviations from a multiyear mean based on the FSU analysis.

Figure 1 shows the zonal wind stress deviation along the equator from October 1996 to June 1997 for the 16 different resolutions. In the high-resolution cases there was a variety of

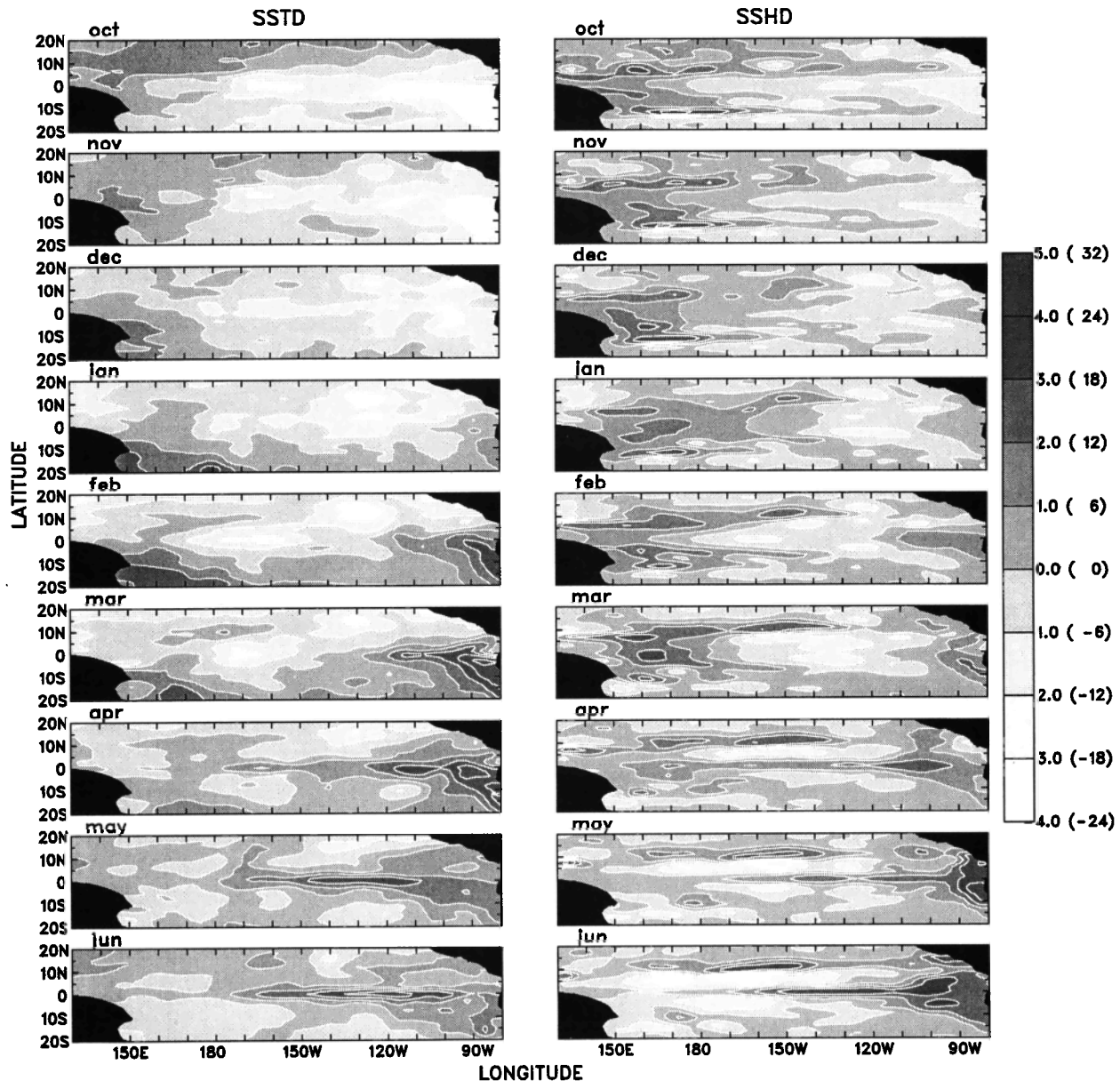


Figure 4. Same as Figure 3, except from the model experiment with the wind forcing of the highest resolution (1° and 1 day).

variabilities in both time and space, among which the most prominent were the westerly wind bursts in the western and central equatorial Pacific. These wind bursts were smeared by the temporal smoothing, especially when the averaging period is longer than 10 days. The spatial smoothing did not change the appearances of the wind bursts, but on scales larger than 5° it did reduce considerably their intensity. A simple pattern of wind variability emerged after the monthly averaging, which consists of three broad westerly wind events centered in December, March, and June and a weak westward propagating signal corresponding to the annual cycle.

To further explore the spatial distribution of the wind variability, the standard deviation of the wind stress magnitude is displayed in Figure 2 for the tropical Pacific Ocean. In the case with the highest resolution (1° in space and 1 day in time), large variance occurred in the western tropical Pacific, especially off the equator, and also in the Intertropical Convergence Zone

(ITCZ). Despite the rather strong equatorial westerly wind bursts shown in Figure 1, the largest variance was not found at the equator. The temporal smoothing greatly reduced the variance but with a much slower rate in the ITCZ and in the northwest corner of the shown basin. These are the regions known for large seasonal wind fluctuations. Therefore the high-frequency winds were responsible for a large portion of the wind variability, except in the regions where the seasonal cycle dominated. The spatial smoothing is generally not as effective as the temporal smoothing in reducing the variance, indicating that high-frequency variations had rather large spatial scales.

3.2. Model/Observation Comparison

In order to establish the credibility of our model, we need to demonstrate that the model could do a decent job, at least in the case where high-resolution wind forcing was applied. Here

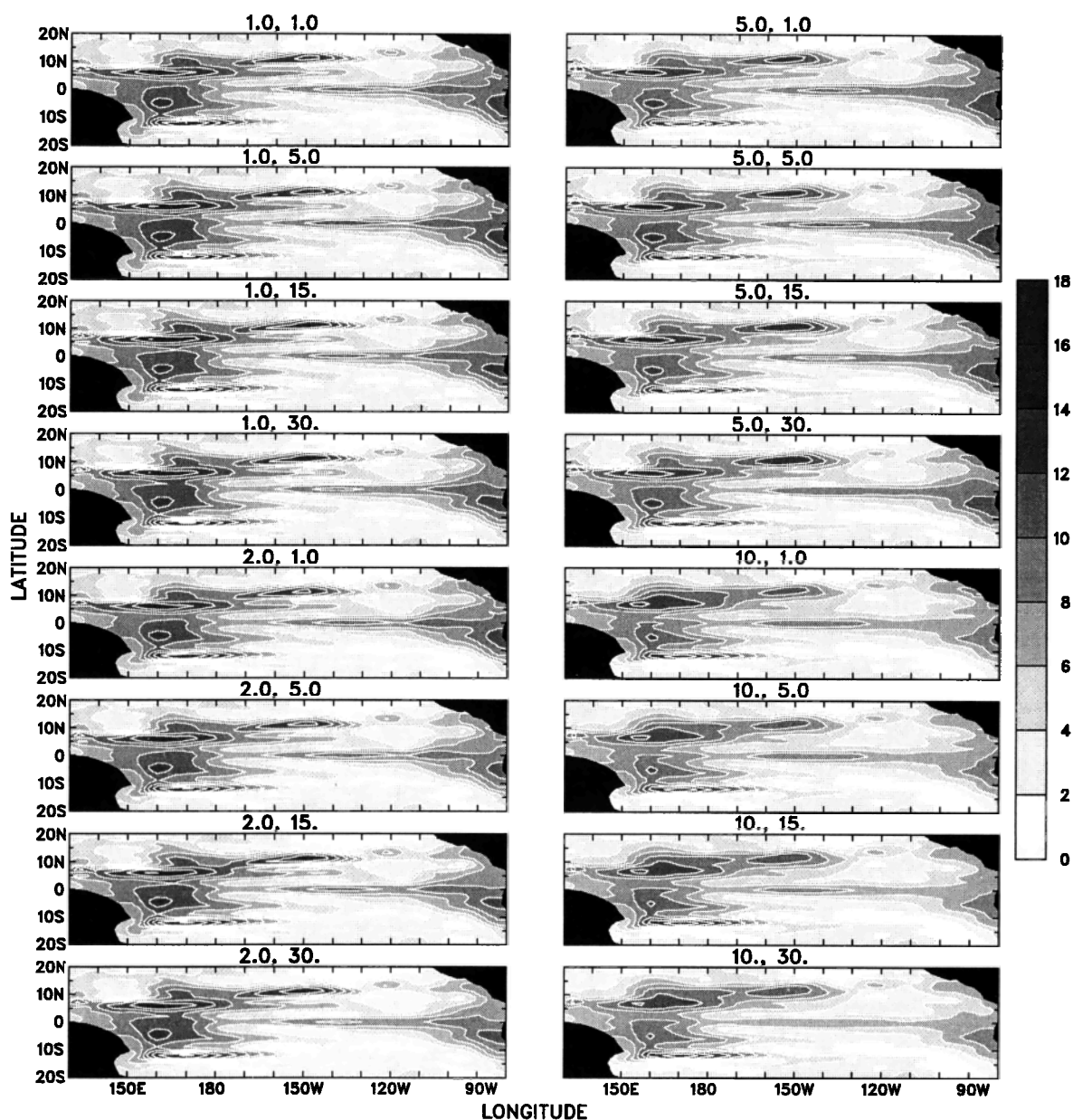


Figure 5. Standard deviation of the model sea level from the 1993–1995 three-year mean for 16 cases with different wind resolutions. The two numbers at top of each plot denote the resolution of wind forcing as in Figure 1.

we choose to compare observed SST and sea level fields with those produced in the experiment with the wind forcing of the highest resolution (1° in space and 1 day in time). This experiment is then used later as the standard case for the sensitivity study. For simplicity and consistency, SST and sea level variations are used throughout this paper to represent the thermal and dynamical ocean responses, respectively.

Figure 3 shows the observed monthly mean deviations of SST and sea level for each month from October 1996 to June 1997. The SST data were blended from ship, buoy, and satellite observations [Reynolds and Smith, 1994], and the sea level data were derived from TOPEX/POSEIDON altimetry. The deviations were calculated relative to the 1993–1995 three-year mean. The largest SST variations appeared in the eastern equatorial and coastal regions. From October to March the SST there changed from a relatively cold state to a warm one, with an

increase of up to 6°C , which is just part of the normal annual cycle. After March, however, the SST did not decrease as dictated by the annual cycle. It remained warm and the zonal extent of the warm water became increasingly larger, indicating the arrival of the 1997/1998 El Niño. The sea level was anomalously high in the western part of the ocean up to March, and then the positive anomalies propagated rapidly to the east. The El Niño was apparently associated with the sea level rising or, equivalently, the thermocline deepening, in the eastern Pacific Ocean.

The corresponding SST and sea level fields from the model are displayed in Figure 4. The overall pattern and evolution of the SST fields are quite similar to those observed, though some errors can be discerned. In particular, the seasonal variation of SST was truthfully reproduced by the model, but the El Niño signal was somewhat underestimated. There was not enough warming near the eastern boundary in May and June. The sea

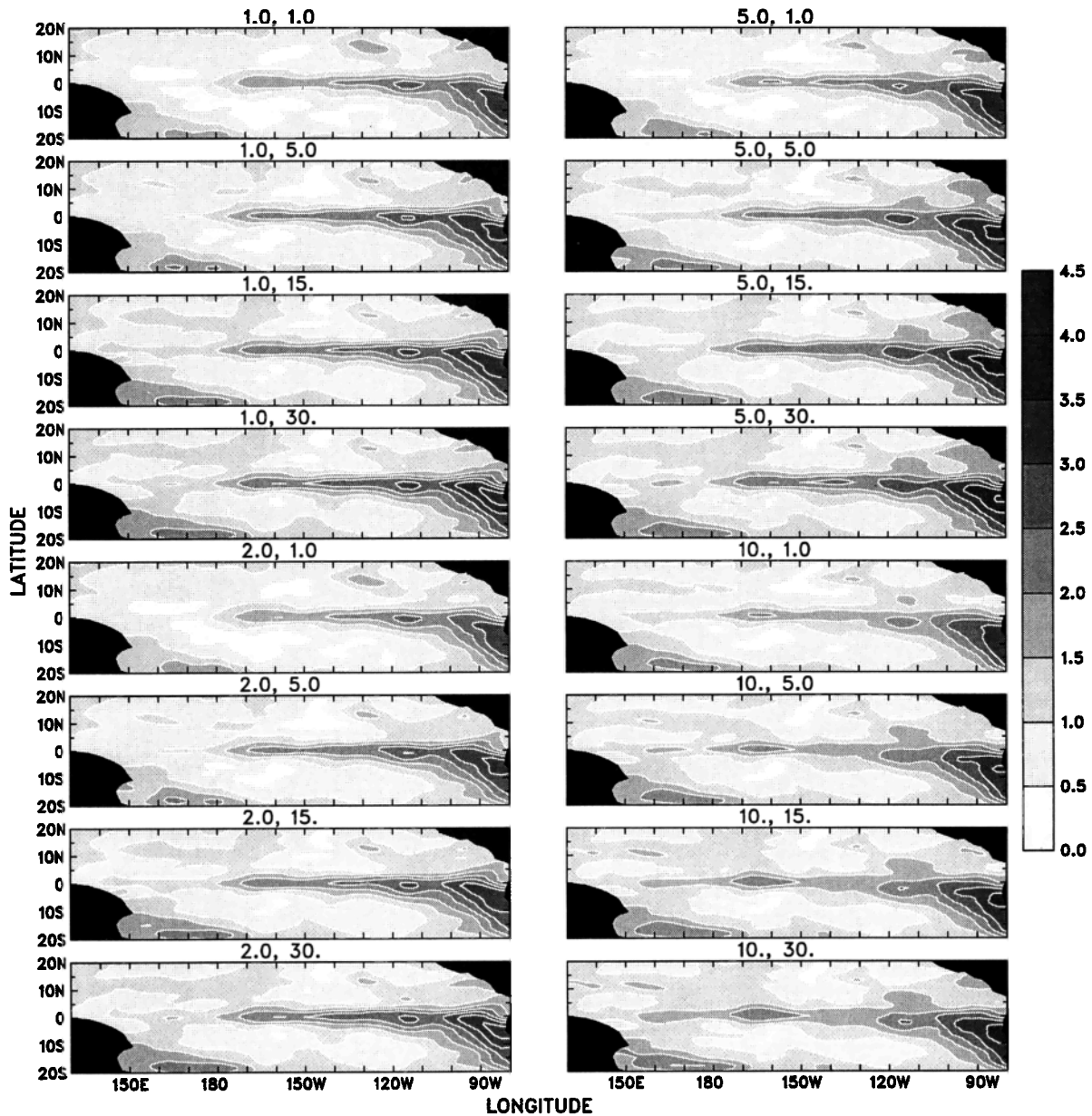


Figure 6. Same as Figure 5, except for SST.

level fields produced by the model did not agree with observations in every detail, but the model simulated well the sequence of the large-scale fluctuation, i.e., the anomalously high sea level first in the west and then in the east and the fast transition in between. Generally speaking, the model was able to capture the observed variabilities of both dynamical and thermal fields during this period. It is fair to conclude that this model is realistic enough for the present study.

3.3. Sensitivity to Wind Resolution

The dynamical model responses to the wind forcing with 16 different resolutions are first compared in Figure 5 in terms of the standard deviation of sea level. Despite the large differences in the wind-forcing variance (Figure 2), the model sea level variances are rather similar for the different experiments. In all cases there are two major centers of activity, one in the west, due to the sea level buildup before the El Niño, and the other in the east, associated with the onset of the El Niño. It is

worth noting that the pattern of the sea level variance is totally different from that of the wind forcing, and thus the ocean dynamical response to the wind is not local. The relatively high variance along the equator and in the eastern part of the ocean, where wind variance was rather small, was mostly a result of the equatorial Kelvin waves. The temporal smoothing of winds with averaging periods up to 1 month had no noticeable effects on the total sea level response. The spatial smoothing, however, made a relatively strong impact on the sea level response in the eastern equatorial Pacific, with approximately 15% and 30% variance reduction for winds averaged over 5° and 10° squares, respectively.

The standard deviations of SST (Figure 6) also have a pattern that is similar in all cases but bears no resemblance to that of the wind forcing. The large variance along the equator and in the east was mainly caused by a combination of the seasonal SST variation and the El Niño (see Figure 3). Because the SST

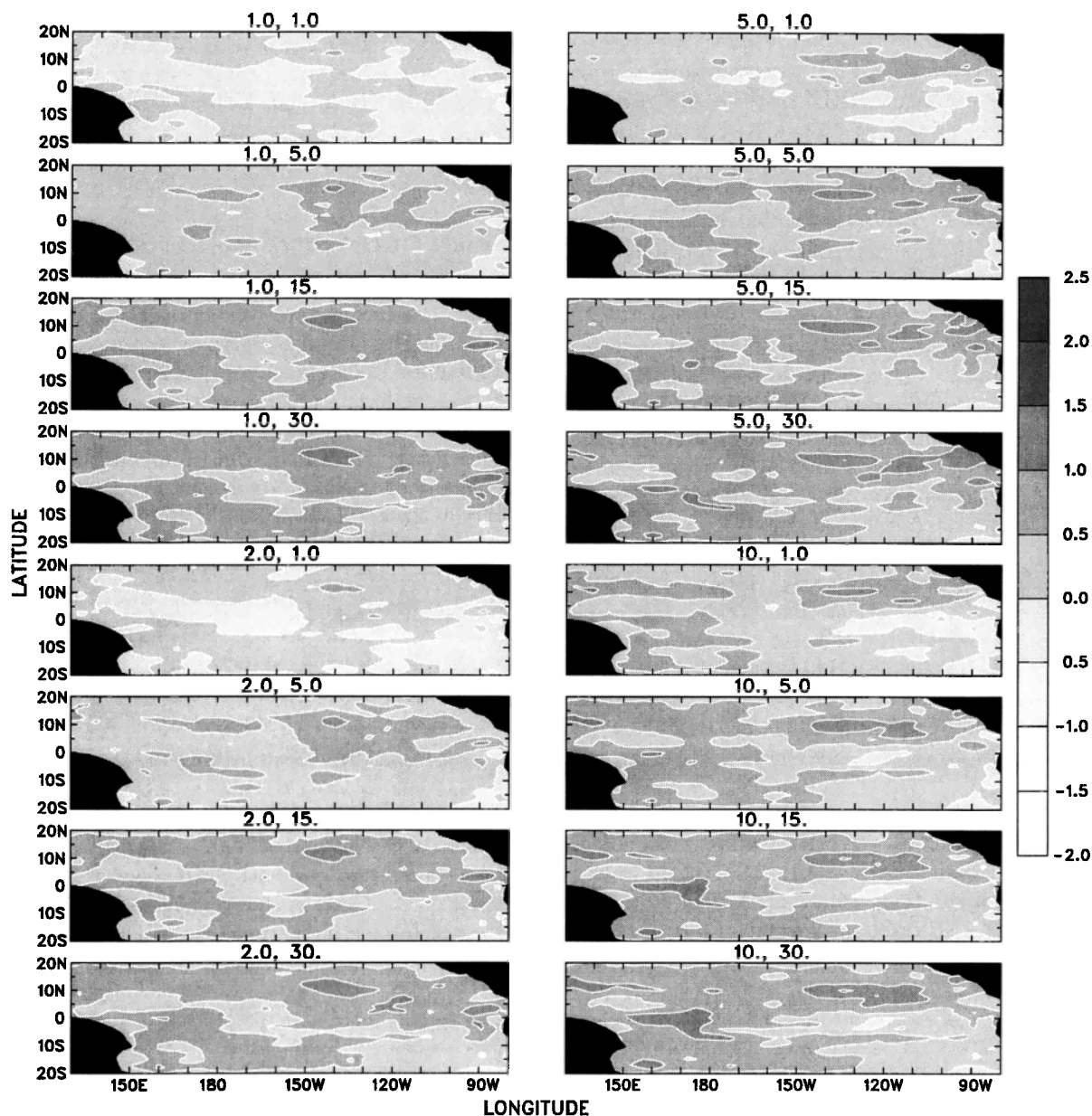


Figure 7. Nine-month average of model SST difference from observation for 16 cases with different wind resolutions.

seasonal cycle there is largely determined by local heat fluxes and local winds [Chen *et al.*, 1994b; Kessler *et al.*, 1998], we should not directly relate the eastern Pacific SST variability to the similar pattern found in sea level, which was remotely wind driven. Indeed, the sensitivity of SST to the wind forcing was quite different from that of sea level. The temporal smoothing now had a more significant impact on the SST variance than the spatial smoothing. The longer the averaging period of winds is, the larger the SST variance. Nearly 30% variance increase was found in the eastern equatorial Pacific for the monthly averaged wind forcing. This is because the smoothing of high-frequency winds reduced vertical mixing and thus resulted in warmer SST and because this effect is especially strong during the warm months when the surface mixed layer was shallow.

From what we have learned about the distribution of high-frequency winds (Figure 2), we would expect the warming

effect by temporal smoothing to be strong off the equator. The SST variance shown in Figure 6 is not a good measure of the average warming effect, which is better evaluated in Figure 7, where the 9-month mean SST differences from observations are depicted. In the case with the highest wind resolution the SST errors were less than 0.5° everywhere. The temporal smoothing caused a warming throughout the basin, generally with larger effect in the off-equatorial regions where high-frequency wind variability is strong. The mean SST was 0.5° to 1° too warm in the cases of monthly averaged winds. The warming pattern does not completely agree with that of the filtered high-frequency winds because vertical mixing also depends on other factors such as the mean mixed layer depth and the temperature gradient below the mixed layer. The spatial smoothing on scales larger than 5° also had a warming effect over most of the basin, especially in the ITCZ, but it seemed to have a cooling tendency in the eastern equatorial Pacific.

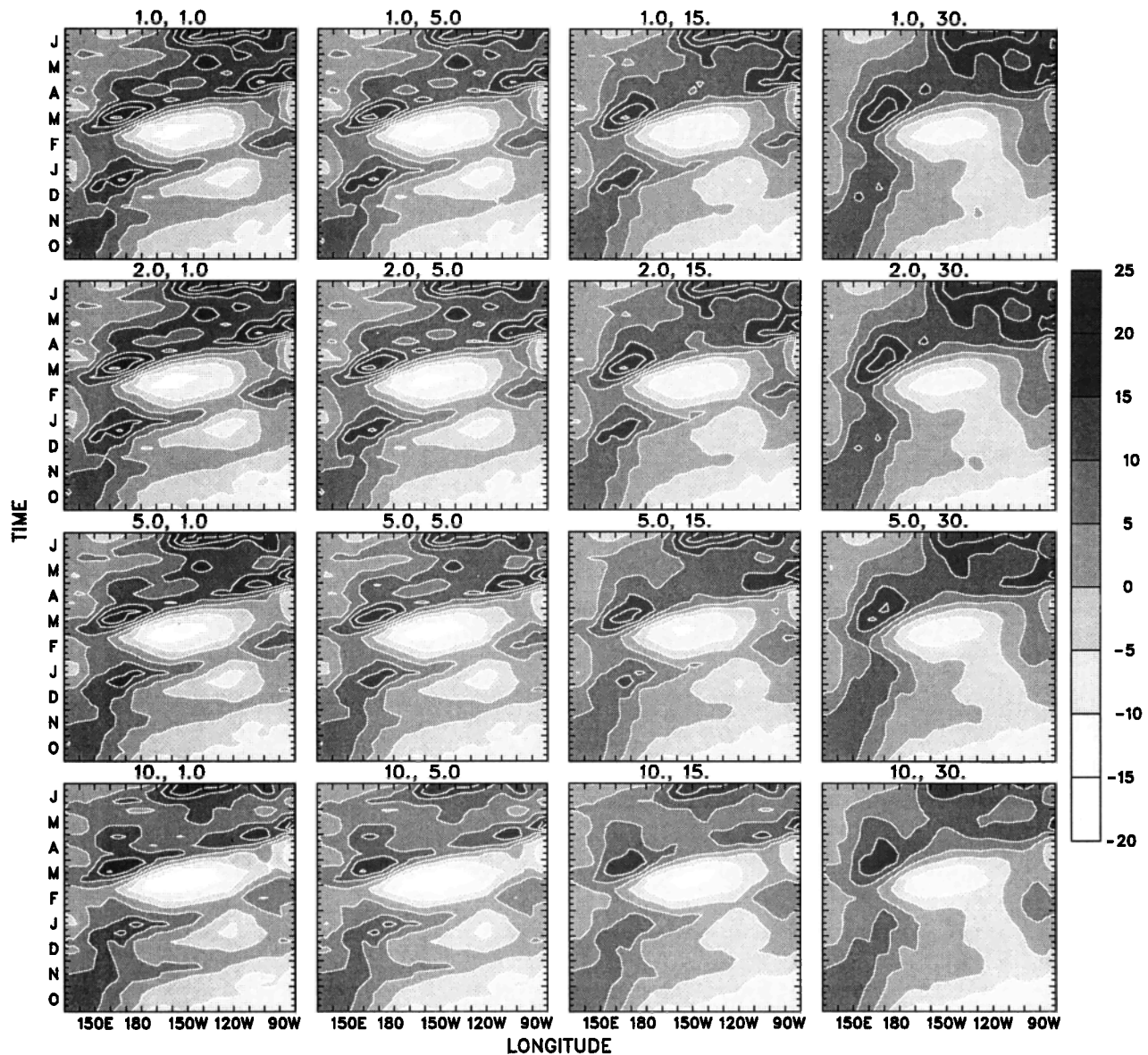


Figure 8. Longitude-time plots of model sea level deviation along the equator for 16 cases with different wind resolutions.

Figure 8 displays the 9-month evolution of the equatorial sea level deviations in response to the different wind forcing. In comparison with Figure 1, it is clear that the dynamical response of the equatorial ocean was essentially a series of downwelling Kelvin waves generated by the westerly wind events. The magnitude of these waves was modified by the local winds as they propagated eastward. The spatial and temporal smoothing of winds on scales of 5° and 5 days or less had little effects on the sea level response. However, the temporal smoothing on longer timescales did affect the sea level evolution considerably. It made the Kelvin waves less intense but the train of waves persist longer, therefore altering the instantaneous sea level fields while retaining the total sea level change. This explains what we have seen in Figure 5; the total sea level variance during this period was not affected by the temporal smoothing of winds. The opposite is true for the spatial wind smoothing on larger scales, which did not have much effect on

the time history of the Kelvin waves but reduced their average magnitude and thus the total variance of sea level.

The corresponding evolution of the equatorial SST deviations is shown in Figure 9. Here the propagation of the Kelvin waves is no longer obvious because SST is strongly affected by local forcing. For example, the large warming in March and April in the eastern equatorial Pacific was mainly a result of the seasonal heat flux increase due to reduced cloud cover. However, the warming after the seasonal peak, namely, the onset of the El Niño, was clearly associated with the sea level rising (thermocline deepening) caused by the series of downwelling Kelvin waves from the western and central equatorial Pacific. Consistent with what we have seen in Figures 6 and 7, the temporal wind smoothing made SST warmer by reducing the energy input for vertical mixing. This effect is most pronounced in the eastern equatorial Pacific during the warm months, though only a relatively small amount of high-

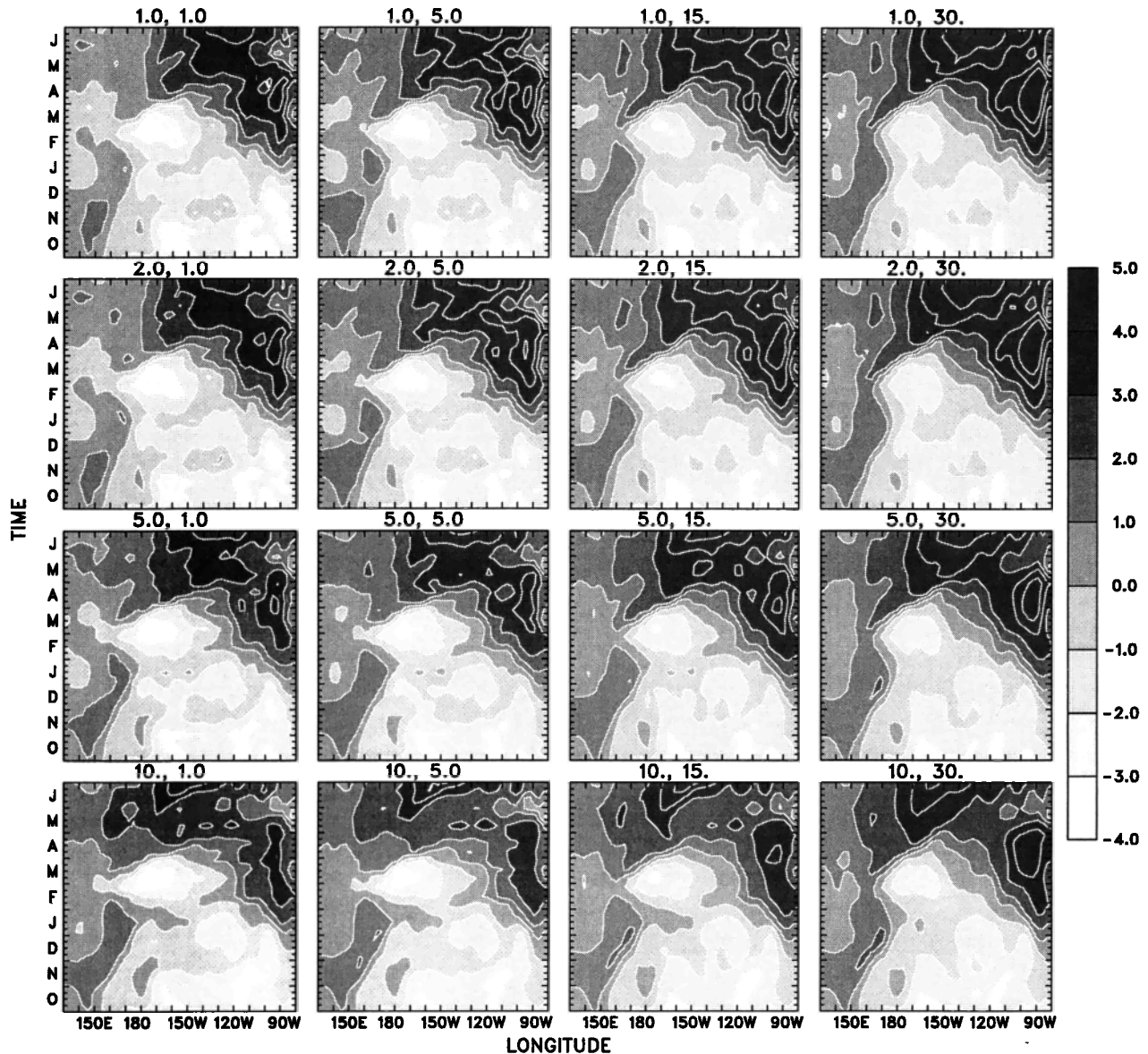


Figure 9. Same as Figure 8, except for SST.

frequency winds was averaged there. The high sensitivity is due to the shallow mixed layer and the large temperature gradient below the mixed layer. The spatial smoothing of winds on scales above 5° actually made SST cooler in the eastern equatorial Pacific, apparently owing to reduced strength of the downwelling Kelvin waves (see Figure 8).

4. Summary and Discussion

We have simulated the tropical Pacific Ocean variability during the onset phase of the 1997/1998 El Niño, with emphasis on the influence of the temporal and spatial resolution of wind forcing. A total of 16 experiments were performed using the NSCAT wind data smoothed at time intervals from 1 to 30 days and on spatial scales from 1° to 10° . The model simulation compared favorably with observations when the high-resolution wind forcing was applied, and it was affected by the temporal and spatial smoothing of winds in different ways.

A major effect of the temporal wind smoothing is to warm

SST by reducing the vertical turbulent mixing. This effect increases as the temporal resolution of winds decreases and is generally more important in regions with larger high-frequency wind activity, except in the eastern equatorial Pacific where extra sensitivity results from the shallow mixed layer and the near-surface thermocline. When the daily wind forcing was replaced by the monthly average, the mean SST increased by 0.5° to 1° over most of the tropical Pacific. Because the distribution of the high-frequency winds is not spatially uniform and does not coincide with that of the mean winds, it would be unrealistic to parameterize their effects by setting a constant lower limit for wind speed or by using a larger drag coefficient for the mean wind stress.

The temporal smoothing of winds also modifies the dynamical ocean response, but the influence is mostly on the instantaneous rather than mean fields. As expected, the intraseasonal variability associated with the equatorial Kelvin waves was largely reduced by the monthly average of wind forcing.

For some relatively weak and isolated wind events, such as the westerly wind bursts in November and December 1996, the monthly averaging was so severe that the winds were no longer able to excite energetic Kelvin waves. However, for stronger and more organized wind events, such as the series of westerlies starting in March 1996, the monthly averaging reduced the amplitude of the Kelvin waves but did not diminish the collected effect of these waves. This probably explains why some models can successfully predict the 1997/1998 El Niño by just using the monthly winds for initialization [e.g., Chen *et al.*, this issue].

On the other hand, because of the relatively large spatial scales of winds, the spatial smoothing was not as effective as the temporal smoothing in reducing the wind energy, and thus its tendency to warm SST was generally smaller. Not only that, the spatial smoothing on scales above 5° actually had a cooling effect in the eastern equatorial Pacific, which made the onset of the El Niño less intense in the model. This effect is caused by the reduced thermocline deepening resulting from decreased downwelling Kelvin waves. Although the spatial smoothing had little effect on the appearances of these waves, it did reduce their amplitude. Here an important spatial scale is the width of the equatorial waveguide in which winds are most effective in generating the Kelvin waves. The difference between the spatial and temporal smoothing is that for a wind event centered near the equator, the former leaks energy out of the waveguide while the latter keeps it within and redistributes it over time.

In order to maintain the influence of the intraseasonal Kelvin waves on the longer-term variabilities such as El Niño, it is more important to preserve their collected energy than their individual characteristics. Therefore, for climate models, the spatial smoothing of wind forcing on scales larger than the width of the equatorial waveguide is a more serious limitation than the temporal smoothing on scales up to 1 month. The onset of the 1997/1998 El Niño can be successfully simulated using the wind forcing averaged to monthly intervals and 2° squares. It should be pointed out that our intention here is to find some general guidance to determine the usable resolution of wind forcing rather than to evaluate the conventional low-resolution wind products. A more objective way for the latter is to construct a wind forcing set by subsampling the NSCAT data at the same time and location as the conventional data and to compare the model responses to the subsampled and the full NSCAT wind forcing.

Acknowledgments. This research was supported by the National Aeronautics and Space Administration through grant JPLCIT 957647 and the National Oceanic and Atmospheric Administration through grants NA56GP0221 and NA76GP0500. We thank the reviewers for their helpful comments on the original manuscript. This is LDEO contribution 5848.

References

- Barnier, B., M. Boukthir, and J. Verron, Use of satellite scatterometer wind data to force a general circulation ocean model, *J. Geophys. Res.*, **96**, 22,025–22,042, 1991.
- Barnier, B., J. Capella, and J. J. O'Brien, The use of satellite scatterometer winds to drive a primitive equation model of the Indian Ocean: The impact of bandlike sampling, *J. Geophys. Res.*, **99**, 14,187–14,196, 1994.
- Bourassa, M. A., M. H. Freilich, D. M. Legler, W. T. Liu and J. J. O'Brien, Wind observations from new satellite and research vessels agree, *Eos Trans. AGU*, **78**, 597–602, 1997.
- Chen, D., and D.-P. Wang, Simulating the time-variable coastal upwelling during CODE 2, *J. Mar. Res.*, **48**, 335–358, 1990.
- Chen, D., L. M. Rothstein, and A. J. Busalacchi, A hybrid vertical mixing scheme and its application to tropical ocean models, *J. Phys. Oceanogr.*, **24**, 2156–2179, 1994a.
- Chen, D., A. J. Busalacchi, and L. M. Rothstein, The roles of vertical mixing, solar radiation, and wind stress in a model simulation of the tropical Pacific seasonal cycle, *J. Geophys. Res.*, **99**, 20,345–20,359, 1994b.
- Chen, D., M. A. Cane, and S. E. Zebiak, The impact of NSCAT winds on predicting the 1997/1998 El Niño: A case study with the Lamont-Doherty Earth Observatory model, *J. Geophys. Res.*, this issue.
- Gent, P. R., The heat budget of the TOGA-COARE domain in an ocean model, *J. Geophys. Res.*, **96**, 3323–3330, 1991.
- Gent, P. R., and M. A. Cane, A reduced gravity, primitive equation model of the upper equatorial zone, *J. Comput. Phys.*, **81**, 444–480, 1989.
- Goldenberg, S. B., and J. J. O'Brien, Time and space variability of tropical Pacific wind stress, *Mon. Weather Rev.*, **109**, 1190–1207, 1981.
- Kessler, W., L. M. Rothstein, and D. Chen, The annual cycle of SST in the eastern tropical Pacific diagnosed in an ocean GCM, *J. Clim.*, **11**, 777–799, 1998.
- Kessler, W. S., M. J. McPhaden, and K. M. Weickmann, Forcing of intraseasonal Kelvin waves in the equatorial Pacific, *J. Geophys. Res.*, **100**, 10,613–10,631, 1995.
- Large, W. G., W. R. Holland, and J. C. Evans, Quasigeostrophic ocean response to real wind forcing: The effects of temporal smoothing, *J. Phys. Oceanogr.*, **21**, 998–1017, 1991.
- Levitus, S. E., Climatological atlas of the world ocean, *NOAA Prof. Pap.*, **13**, 173 pp., U.S. Govt. Print. Off., Washington, D. C., 1982.
- Liu, W. T., W. Tang, and P. S. Polito, NASA Scatterometer provides global ocean-surface wind fields with more structures than numerical weather prediction, *Geophys. Res. Lett.*, **25**, 761–764, 1998.
- Milliff, R. F., W. G. Large, W. R. Holland, and J. C. McWilliams, The general circulation responses of high-resolution North Atlantic Ocean models to synthetic scatterometer winds, *J. Phys. Oceanogr.*, **26**, 1747–1768, 1996.
- Reynolds, R. W., and T. M. Smith, Improved global sea surface temperature analyses, *J. Clim.*, **7**, 929–948, 1994.
- Webster, P. J., and R. Lukas, TOGA-COARE: The coupled ocean-atmosphere response experiment, *Bull. Am. Meteorol. Soc.*, **73**, 1377–1416, 1992.
- M. A. Cane, D. Chen, Y. Kushnir, D. Witter, and S. E. Zebiak, Lamont-Doherty Earth Observatory, Columbia University, Route 9W, P. O. Box 1000, Palisades, NY 10964. (e-mail: dchen@wind.ideo.columbia.edu)
- W. T. Liu, Jet Propulsion Laboratory, Pasadena, CA 91109.

(Received March 27, 1998; revised September 17, 1998; accepted September 23, 1998.)